International Journal of Advances in Engineering and Management (IJAEM)
Volume 3, Issue 7 July 2021, pp: 1279-1289 www.ijaem.net ISSN: 2395-5252

# Investigation on the Stress Distributions in a Thick-Walled Cylinder with Internal Pressure.

[*]Amodu, O. A., [**]Adamu, A. A. and [*]Anikoh, G. A.

[*]*Department of Mineral and Petroleum Resources Engineering, School of Engineering,Kogi State Polytechnic, Lokoja, Itapke Campus, Kogi State Nigeria.*

[**]*Department of Civil Engineering, School of Engineering, Kogi State Polytechnic, Lokoja.*

Submitted: 25-06-2021 Revised: 06-07-2021 Accepted: 09-07-2021

**ABSTRACT**

The concept of thick cylinders with internal pressure is complex and an area of great interest. It involves analyzing the pressure exerted on the cylinder and the accompanying stresses and strains that arise as a result of the pressure. In this research, strains related to selected points on a pressurized thick cylinder were measured using strain gauges positioned at the selected points. The circumferential and radial stresses were calculated from the strain readings. The graphical and boundary conditions of intercept, A and slop B was calculated and compared with the internal pressure, P, which shows a linear increase as the depth of penetration increases. It was deduced from the calculated percentage errors of A and B that the errors obtained during the course of this study was within the permissible range of 15%. It was concluded that at a high pressurized pressure, the circumferential stress increases in the inner surface and expands outwardly thereby becoming thinner in terms of the diameter. The radial stress also increases with a minus sign indicating a compressive radial stress. This experiment can be used satisfactorily to analysis internal crack of a cylinder.

**Keywords:** boundary, cylinder, circumferential, pressurized, radial, thick

## I. INTRODUCTION

When an internal pressure is exerted on a closed cylindrical shell by a fluid under pressure, stresses are produced in the shell. A circumferential or hoop stress is developed if the wall expands and increases the volume of the cylinder. Also, longitudinal and radial stresses develop: longitudinal stress as a result of the pressure at the ends of the cylinder that cause an increase in the length and radial stress as a result of pressure acting at right angles to the surface thereby squashing the wall of the shell.

Radial stress is highest at the inner wall surface and has a value equal to the gauge pressure (P) at the inner surface. The stress reduces outwards till it gets to zero at the outer surface of the cylinder.

If the ratio of the wall thickness to the internal diameter of the cylindrical shell is greater than 1/20, the stress is significant hence the radial stress is important and must be noted. Such a cylinder is referred to as a thick cylinder(Kadir)

Pressure vessels have a widespread application in the industrial sector. Pressure vessels in form of pipes, tanks, heat exchangers, separators and a host of others are used for different industrial processes in key industrial sectors of the economy like oil, petrochemical and nuclear. Evaluation of the distribution of stress in internally-pressured vessels is important and mandatory to ensure the structural integrity of the vessels and ultimately safety(Annaratone, 2010).

Pipes are most widely used pressure vessels which are used extensively to convey fluids from one place to another. Usually of hollow cylindrical structure, pipes are manufactured from carbon steel, cast or ductile iron, polyvinyl chloride, polyethylene etc.and are used extensively in the petrochemical, refinery, and pipeline industries, water distribution, manufacturing and production amongst others. Pipes are widely available, inexpensive, and maintainable. However, these materials are liable to failures like cracking, pitting, local wall thinning, which can be generated by corrosion, erosion and environmental exposure to various substances(Nascimento, 2009).

A thick-walled cylinder is one in which the thickness of the wall is greater than one-twentieth of the radius. The principal stresses that exist in an internally pressurized thick cylinder are the longitudinal or axial ($\sigma_L$), the circumferential or hoop ($\sigma_h$) and the radial stress ($\sigma_r$). The difference between a thick and thin cylinder is that thin cylinders do not have the radial stress component.

International Journal of Advances in Engineering and Management (IJAEM)
Volume 3, Issue 7 July 2021, pp: 1279-1289 www.ijaem.net ISSN: 2395-5252

Radial stress becomes important when the thickness of the pipe wall becomes greater than one-twentieth of the diameter (Dunn).

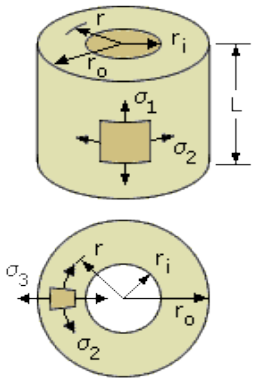


Figure 1: Stress and strain distribution in a thick cylinder (Source: www.fea-optimization.com )

Lame's theory forms the basis for the analysis of stress and strain distribution in thick cylinders. He derived the formula in1833 using the stress system show in figure 2(Jaeyoung Lee, 2012).

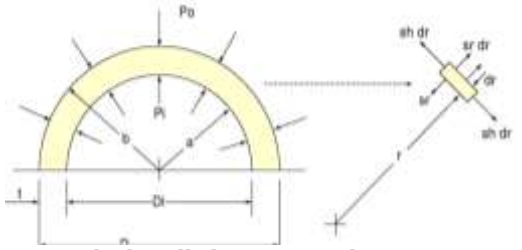


Figure 2: Thick walled pipe stress diagram (Source: www.offshore-mag.com)

Consider the thick cylinder shown in figure 3a and stresses acting on an element of unit length at radius r represented as shown in figure 3b below.

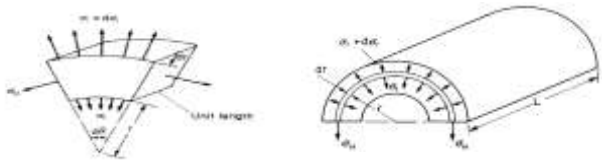

Figure 3 (a) Internally pressurized thick cylinder and (b) Unit element of thick cylinder (Source: (E.J.Hearn, 1977))

The radial stress increasing from $\sigma_r$ to $\sigma_r + d\sigma_r$over the element thickness$d_r$stresses are assumed tensile and the radial equilibrium of the element is given as:

$$(\sigma_r + d\sigma_r)(r + dr)d\theta \times 1 - \sigma_r \times rd\theta \times 1 = 2\sigma_H \times dr \times 1 \times \sin\frac{d\theta}{2} \dots\dots\dots\dots 1$$

For small angles,

$$\sin\frac{d\theta}{2} \cong \frac{d\theta}{2} \text{radian} \dots\dots\dots\dots\dots\dots\dots\dots\dots\dots 2$$

Neglecting second order small quantities, we obtain:

$$rd\sigma_r + \sigma_r dr = \sigma_H dr$$

$$r\frac{d\sigma_r}{dr} = \sigma_H - \sigma_r \dots\dots\dots\dots\dots\dots\dots\dots\dots\dots\dots 3$$

Assuming plane section remains, constant strain will then be constant across the wall of the cylinder. Therefore:

$$\varepsilon_L = \frac{1}{E}[\sigma_L - \nu\sigma_r - \nu\sigma_H]$$

$$\text{constant} = \frac{1}{E}[\sigma_L - \nu(\sigma_r - \sigma_H)] = 2A$$

Also if longitudinal stress $\sigma_L$ is constant, then:

$$\sigma_r + \sigma_H = \text{constant} = 2A \dots\dots\dots\dots\dots\dots\dots\dots\dots\dots 4$$

Substituting in 3 for $\sigma_H$

$$2A - \sigma_r - \sigma_r = r\frac{d\sigma_r}{dr} \dots\dots\dots\dots\dots\dots\dots\dots\dots\dots 5$$

Multiplying by r and rearranging we obtain:

$$2\sigma_r r + r^2\frac{d\sigma_r}{dr} - 2Ar = 0$$

$$\frac{d}{dr}(\sigma_r r^2 - Ar^2) = 0 \dots\dots\dots\dots\dots\dots\dots\dots\dots\dots 6$$

Integrating yields,

$$\sigma_r r^2 - Ar^2 = \text{constant} = -B$$

$$\sigma_r = A - \frac{B}{r^2} \dots\dots\dots\dots\dots\dots\dots\dots\dots\dots 7$$

And from equation 4

$$\sigma_H = A + \frac{B}{r^2} \dots\dots\dots\dots\dots\dots\dots\dots\dots\dots 8$$

Equations 7 and 8 allow the radial and hoop stress at any radius to be determined in terms of constants A and B. For any pressure condition, there will always be two known conditions of stress, which

International Journal of Advances in Engineering and Management (IJAEM)
Volume 3, Issue 7 July 2021, pp: 1279-1289 www.ijaem.net ISSN: 2395-5252

makes it possible for the constants to be determined.

Considering the thick cylinder below

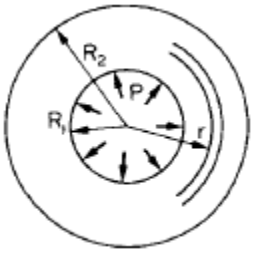


Figure 4: Cross section of a cylinder

If subjected to an internal pressure P, with external pressure being zero, the conditions of stress at which Lame's constants A and B can be determined are at;

$$r = R_1 : \ \sigma_r = -P \text{ and } r = R_2 : \ \sigma_r = 0$$

Internal stress is considered negative radial since it produces radial compression (E.J.Hearn, 1977).

Substituting the conditions in (7) yields:

$$-P = A - \frac{B}{R_1^2} \ldots\ldots\ldots\ldots\ldots\ldots\ldots\ldots\ldots\ldots\ldots$$

$$\ldots\ldots\ldots\ldots\ldots\ldots\ldots\ldots 9$$

$$0 = A - \frac{B}{R_2^2} \ldots\ldots\ldots\ldots\ldots\ldots\ldots\ldots\ldots\ldots\ldots$$

$$\ldots\ldots\ldots\ldots\ldots\ldots\ldots\ldots\ldots 10$$

Therefore:

$$A = \frac{PR_1^2}{(R_2^2 - R_1^2)} \text{ and } B = \frac{PR_1^2R_2^2}{(R_2^2 - R_1^2)} \ldots\ldots\ldots\ldots\ldots\ldots\ldots$$

$$\ldots\ldots\ldots\ldots\ldots\ldots\ldots\ldots 11 \text{ (a)and (b)}$$

Where P = Internal Pressure

$R_1$ = Internal Radius

$R_2$ = External Radius

## II. METHODOLOGY

### 2.1 Description of apparatus

The apparatus described below were used for the for the research work.

A thick-walled aluminum cylinder with outer radius $R_O$=152mm and inner radius $R_i$ =77.5mm, held in a robust frame.

10 strain gauges set at intervals of 12.5mm on the lateral surface of the cylinder. These gauges measured the radial and hoop strains.

An 8 ton hydraulic arm used to provide the internal pressure (P) by forcing a tapered plug into the bore of the cylinder.

A hydraulic cylinder that holds the oil used to lubricate the contact area between the tapered plug and the bore in the cylinder, to reduce the frictional force acting between the inner and outer cylinder.

A solatron Stumberger 3530 Data Logger into which the strain gauge results were fed and from which direct readings in micro-strain were produced.

A tapered plug which was rammed into the cylinder to pressurize it internally.

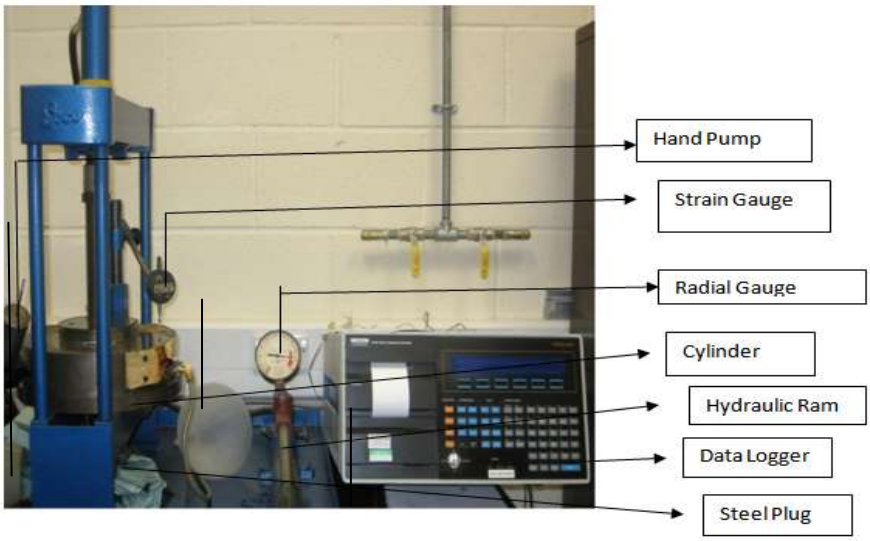


FIGURE 5: THICK CYLINDER AND DATA LOGGER.

International Journal of Advances in Engineering and Management (IJAEM)
Volume 3, Issue 7 July 2021, pp: 1279-1289 www.ijaem.net ISSN: 2395-5252

**2.2 Procedure**

The lubricating or hand pump was filled with lubricating oil and the oil was pumped while the tapered plug was rotated simultaneously to ensure equal lubrication until the spiral groove was filled with the oil and the tapered plug was properly lubricated. A zero reference was attained for the dial readings.

An initial weight was applied by the hydraulic ram forcing the tapered plug into the hole or ring in the thick cylinder and an initial reading of 0.3mm was obtained. The dials were set at zero and 10 channels of strain were logged into the data logging system, and the experiment commenced.

The hydraulic ram was stroked while lubrication was done simultaneously with the aid of the lubricating or hand pump so as to ensure uniformity between the oil pump and the ram. The strain readings were taken initially at 0.75mm.

The procedure was repeated at an increment of 0.75 until a penetration depth of 3.91mm was achieved for the fifth penetration. Lubrication was continuously done to ensure the cylinder did not get stuck. The strain readings on 10 channels was taken(in micro strain) at this depth and also for subsequence three increments of plug insertion for up to 4mm

The hydraulic ram was carefully removed whilst holding the spacer bar firmly to avoid any accidental pulling out of the bar up the roof.

Upon completion of the practical, the pressure builds up was relieved via the release valve of the pump and the hydraulic ram.

The hoop and radial stresses were calculated using the strain reading at each penetration depth and corresponding radii.

## III. RESULTS:

| | | DEPTH OF PENETRATION (mm) | | | | |
|---|---|---|---|---|---|---|
| STRAIN | CHANNELS | 0.73 | 1.44 | 2.19 | 2.97 | 3.91 |
| RADIAL | 1 | -8 | -19 | -30 | -47 | -62 |
| | 3 | -11 | -28 | -50 | -69 | -94 |
| | 5 | -17 | -44 | -73 | -103 | -139 |
| | 7 | -25 | -58 | -103 | -147 | -202 |
| | 9 | -37 | -110 | -200 | -264 | -330 |
| HOOP | 11 | 26 | 56 | 92 | 132 | 183 |
| | 13 | 32 | 69 | 110 | 159 | 215 |
| | 15 | 34 | 76 | 127 | 189 | 254 |
| | 17 | 38 | 95 | 262 | 229 | 312 |
| | 19 | 53 | 124 | 210 | 294 | 399 |

Table 1: Strain values at corresponding depths of penetration

3.1 **Stress calculations**

$$\sigma_\theta = \frac{E}{1-\mu^2}\left(\ell_\theta + \mu\ell_r\right)(\text{hoop stress})$$

$$\sigma_r = \frac{E}{1-\mu^2}\left(\ell_r + \mu\ell_\theta\right)(\text{radial stress})$$

Where: Young's modulus$(E) = 208\text{kN/mm}^2$ , Poisson's ratio$(\mu) = 0.3$,$\ell_\theta$ = hoop stain and $\ell_r$ = radial strain.

3.2: Summary of hoop and radial stress results from calculations in tabular and graphical form

| Penetration Depth = 0.73mm | | | | | |
|---|---|---|---|---|---|
| r (mm) | 90.5 | 103 | 115.5 | 128 | 140.5 |
| $1/r^2$ $mm^{-2}$ $(10^{-5})$ | 12.21 | 9.43 | 7.50 | 6.10 | 5.07 |
| $e_\theta$(microstrain) | 26 | 32 | 34 | 38 | 53 |
| $e_r$(microstrain) | -8 | -11 | -17 | -25 | -37 |

International Journal of Advances in Engineering and Management (IJAEM)
Volume 3, Issue 7 July 2021, pp: 1279-1289 www.ijaem.net ISSN: 2395-5252

| | | | | | |
|---|---|---|---|---|---|
| $\sigma_\theta$(N/mm$^2$) | 5.39 | 6.56 | 6.61 | 6.97 | 9.58 |
| $\sigma_r$(N/mm$^2$) | -0.046 | -0.32 | -1.55 | -3.12 | -4.82 |

Table 2.0 Values of δθ and δr at 0.73 penetration depth.

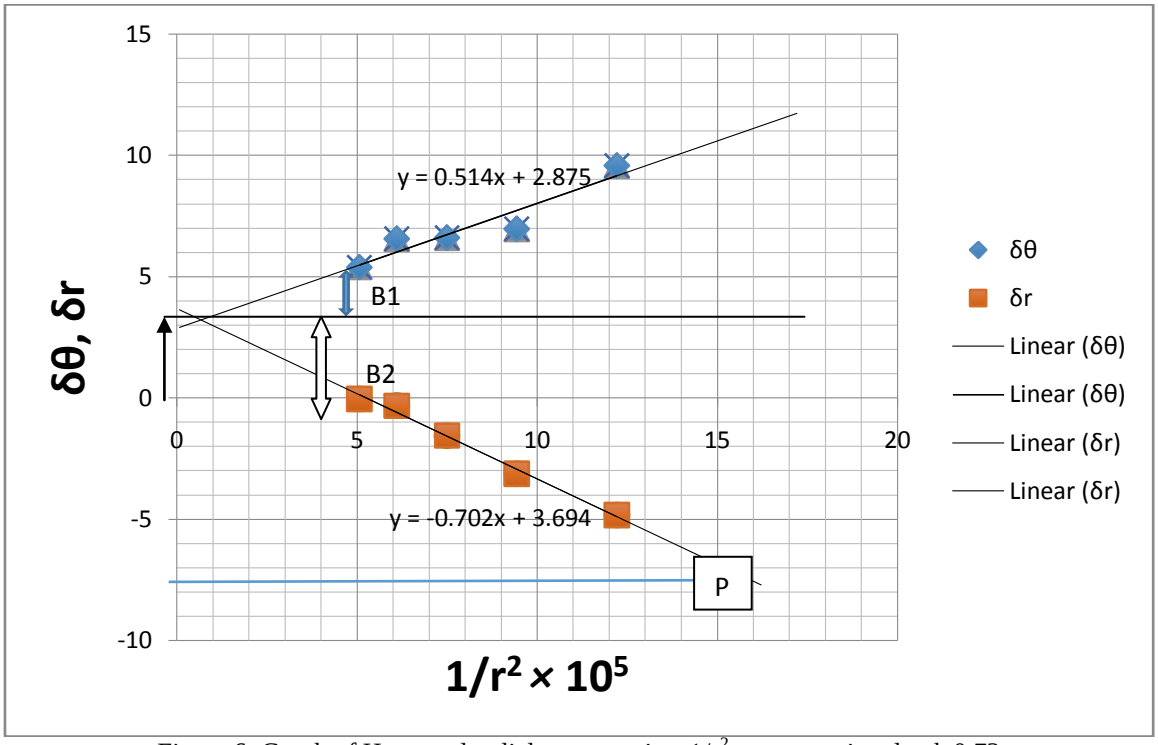


Figure 6: Graph of Hoop and radial stress against 1/r$^2$ at penetration depth 0.73

| | Penetration depth=1.44 | | | | |
|---|---|---|---|---|---|
| r (mm) | 90.5 | 103 | 115.5 | 128 | 140.5 |
| 1/r$^2$ mm$^{-2}$ (10$^{-5}$) | 12.21 | 9.43 | 7.50 | 6.10 | 5.07 |
| $e_\theta$(microstrain) | 56 | 69 | 76 | 95 | 124 |
| $e_r$(microstrain) | -19 | -28 | -44 | -58 | -110 |
| $\sigma_\theta$(N/mm$^2$) | 11.50 | 13.85 | 14.35 | 17.74 | 20.8 |
| $\sigma_r$(N/mm$^2$) | -0.50 | -1.67 | -4.85 | -6.74 | -16.64 |

Table 3.0 Values of δθ and δr at 1.44 penetration depth.

International Journal of Advances in Engineering and Management (IJAEM)
Volume 3, Issue 7 July 2021, pp: 1279-1289 www.ijaem.net ISSN: 2395-5252

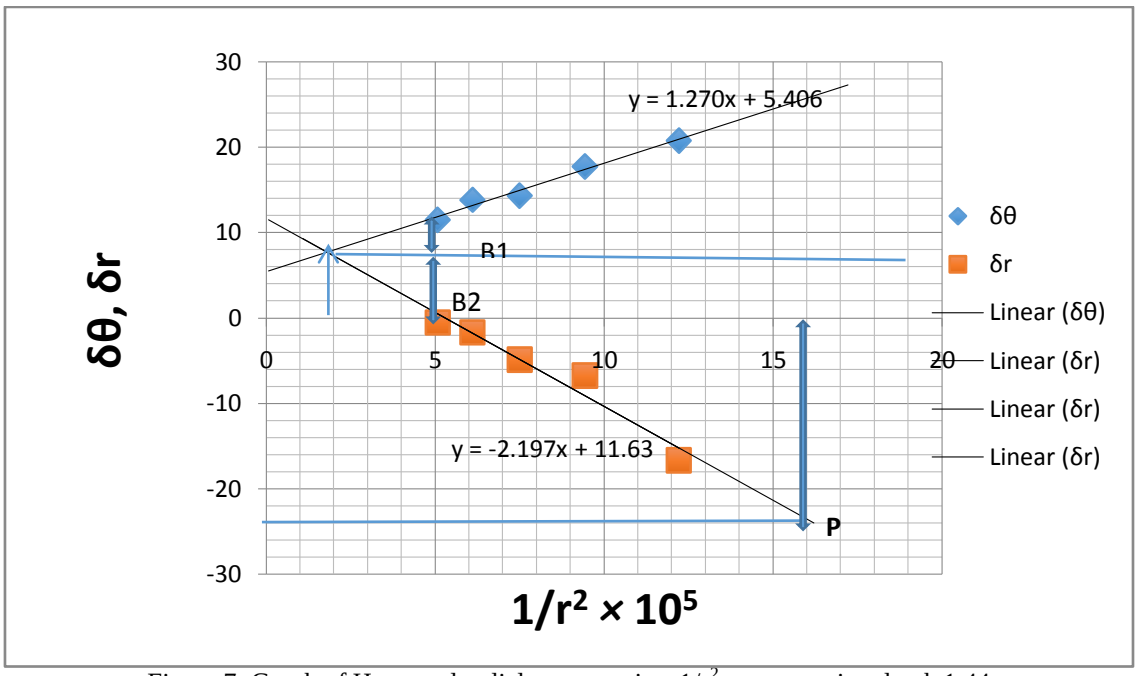


Figure 7: Graph of Hoop and radial stress against $1/r^2$ at penetration depth 1.44

| Penetration Depth = 2.19 mm | | | | | |
|---|---|---|---|---|---|
| r (mm) | 90.5 | 103 | 115.5 | 128 | 140.5 |
| $1/r^2$ $mm^{-2}$ ($10^{-5}$) | 12.21 | 9.43 | 7.50 | 6.10 | 5.07 |
| $e_\theta$(microstrain) | 92 | 110 | 127 | 162 | 210 |
| $e_r$(microstrain) | -30 | -50 | -73 | -103 | -200 |
| $\sigma_\theta$($N/mm^2$) | 18.97 | 21.71 | 24.02 | 29.97 | 34.29 |
| $\sigma_r$($N/mm^2$) | -0.55 | -3.89 | -7.98 | -12.43 | -31.31 |

Table 4.0 Values of δθ and δr at 2.19 penetration depth

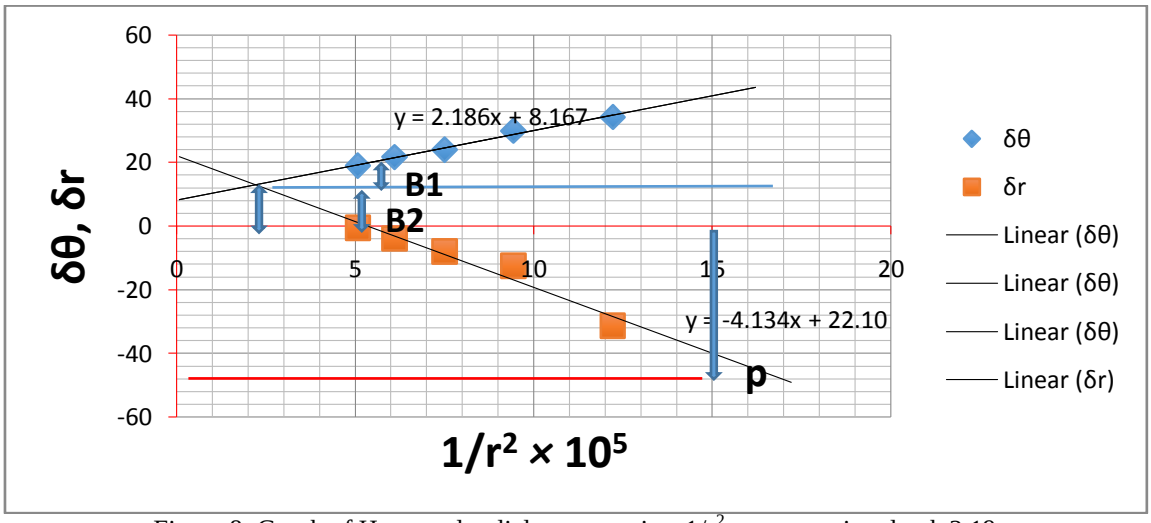


Figure 8: Graph of Hoop and radial stress against $1/r^2$ at penetration depth 2.19

International Journal of Advances in Engineering and Management (IJAEM)
Volume 3, Issue 7 July 2021, pp: 1279-1289 www.ijaem.net ISSN: 2395-5252

| Penetration Depth = 2.97 mm | | | | | |
|---|---|---|---|---|---|
| r (mm) | 90.5 | 103 | 115.5 | 128 | 140.5 |
| $1/r^2$ $mm^{-2}$ $(10^{-5})$ | 12.21 | 9.43 | 7.50 | 6.10 | 5.07 |
| $e_\theta$(microstrain) | 132 | 159 | 189 | 229 | 294 |
| $e_r$(microstrain) | -47 | -69 | -103 | -147 | -264 |
| $\sigma_\theta$($N/mm^2$) | 26.95 | 31.61 | 36.14 | 42.26 | 49.10 |
| $\sigma_r$($N/mm^2$) | -1.69 | -4.87 | -10.58 | -17.90 | -40.18 |

Table 5.0 Values of δθ and δr at 2.97 penetration depth.

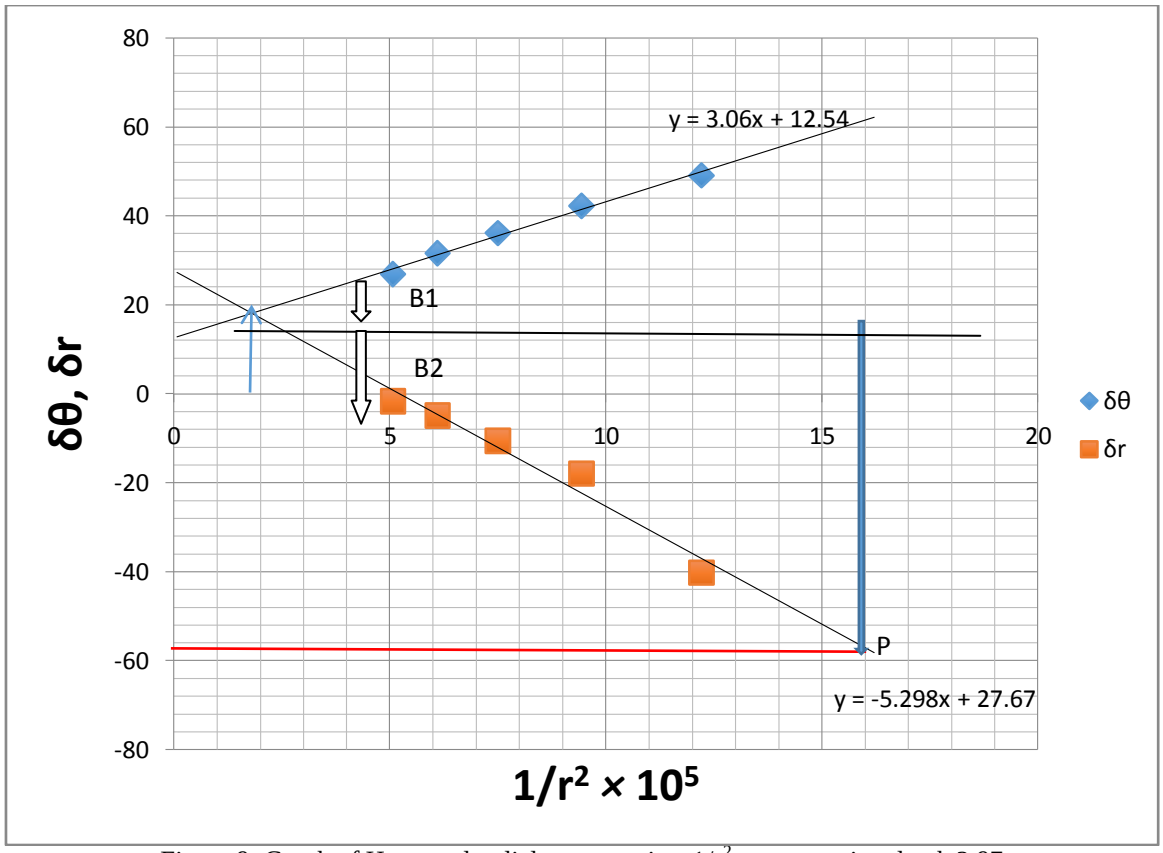


Figure 9: Graph of Hoop and radial stress against $1/r^2$ at penetration depth 2.97

| Penetration Depth = 3.91 mm | | | | | |
|---|---|---|---|---|---|
| r (mm) | 90.5 | 103 | 115.5 | 128 | 140.5 |
| $1/r^2$ $mm^{-2}$ $(10^{-5})$ | 12.21 | 9.43 | 7.50 | 6.10 | 5.07 |
| $e_\theta$(microstrain) | 183 | 215 | 254 | 312 | 399 |
| $e_r$(microstrain) | -62 | -94 | -139 | -202 | -330 |
| $\sigma_\theta$($N/mm^2$) | 37.58 | 42.70 | 48.53 | 57.46 | 68.57 |
| $\sigma_r$($N/mm^2$) | -1.62 | -6.74 | -14.35 | -24.78 | -48.07 |

Table 6.0 Values of δθ and δr at 3.91 penetration depth.

International Journal of Advances in Engineering and Management (IJAEM)
Volume 3, Issue 7 July 2021, pp: 1279-1289 www.ijaem.net ISSN: 2395-5252

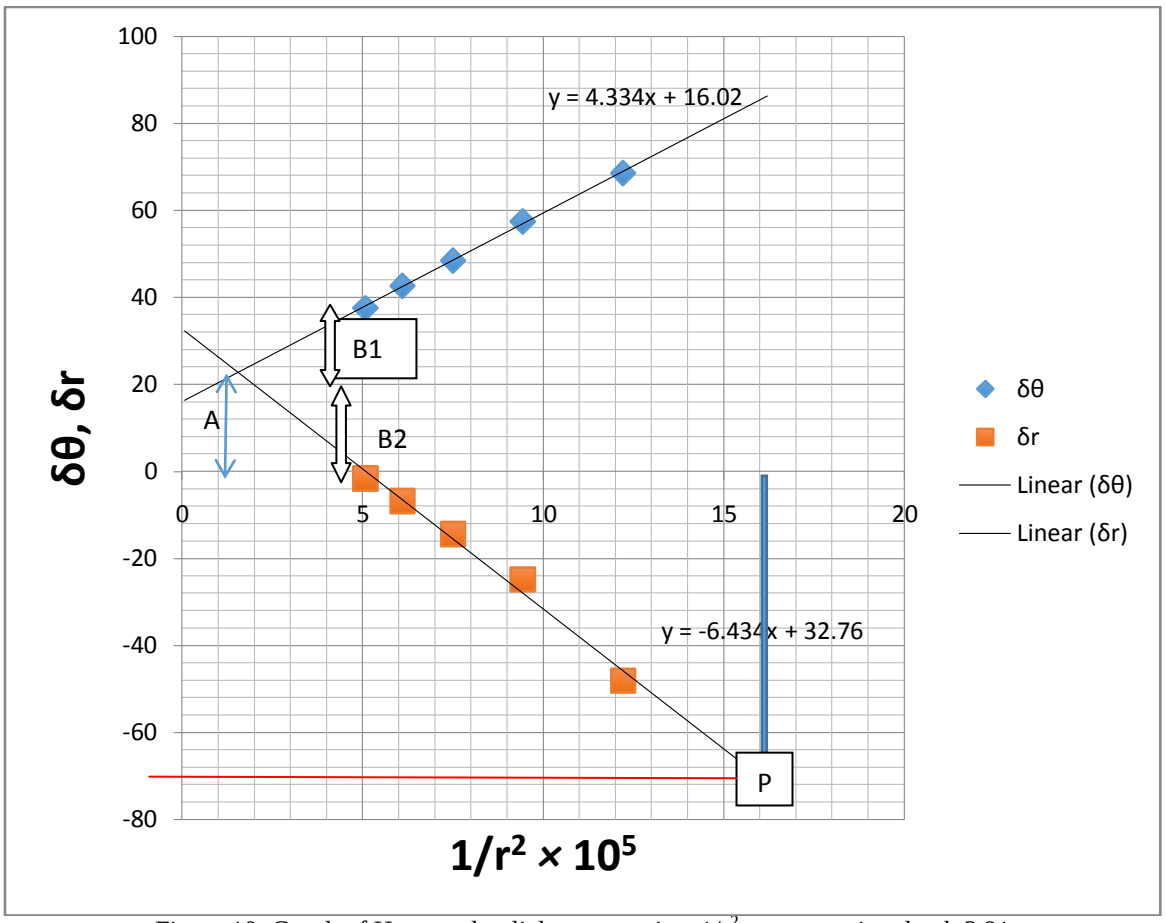


Figure 10: Graph of Hoop and radial stress against $1/r^2$ at penetration depth 3.91

| PENERATION DEPTH (mm) | 0.73 | 1.44 | 2.19 | 2.97 | 3.91 |
|---|---|---|---|---|---|
| A ($N/mm^2$) | 3.1 | 7.9 | 14.0 | 18.0 | 23.0 |
| B (N) | 60860 | 173390 | 316040 | 417945 | 538445 |
| P ($N/mm^2$) | -7.6 | -24.0 | -42.0 | -57.0 | -69.0 |

Table 2: Values of A, B and P obtained from graph

3.3 Using boundary conditions

| PENERATION DEPTH (mm) | 0.73 | 1.44 | 2.19 | 2.97 | 3.91 |
|---|---|---|---|---|---|
| A ($N/mm^2$) | 2.67 | 8.43 | 14.75 | 20.02 | 24.23 |
| B (N) | 61682.96 | 194788 | 340879.52 | 462622 | 560016 |
| P ($N/mm^2$) | -7.6 | -24.0 | -42.0 | -57.0 | -69.0 |

Table 3: Values of A and B obtained from boundary condition

International Journal of Advances in Engineering and Management (IJAEM)
Volume 3, Issue 7 July 2021, pp: 1279-1289 www.ijaem.net ISSN: 2395-5252

| Depths (mm) | GRAPHICAL VALUES | | BOUNDARY CONDITION | | -P (N/mm$^2$) |
|---|---|---|---|---|---|
| | A ( N/mm$^2$) | B (N) | A ( N/mm$^2$) | B (N) | |
| 0.73 | 3.1 | 60680 | 2.67 | 61683 | 7.6 |
| 1.44 | 7.9 | 173390 | 8.43 | 194788 | 24 |
| 2.19 | 14 | 316040 | 14.75 | 340880 | 42 |
| 2.97 | 18 | 417945 | 20.02 | 462622 | 57 |
| 3.91 | 23 | 538445 | 24.23 | 560016 | 69 |

Table 4: The theoretical and experimental values of A and B

| | GRAPHICAL VALUE | | THEORETICAL VALUE | | %Error | |
|---|---|---|---|---|---|---|
| Depth of penetration | A | B | A | B | A | B |
| 0.73 | 3.1 | 60860 | 2.67 | 61683 | 13 | 1.4 |
| 1.44 | 7.9 | 173390 | 8.43 | 194788 | 6.7 | 12.3 |
| 2.19 | 14 | 316040 | 14,75 | 340880 | 5.4 | 7.9 |
| 2.97 | 18 | 417945 | 20.02 | 462622 | 11 | 10.7 |
| 3.91 | 23 | 538445 | 24.23 | 560016 | 5.3 | 4 |

Table 5: percentage error values for A and B

| Penetration Depth = 0.73mm | | | | | |
|---|---|---|---|---|---|
| r (mm) | 90.5 | 103 | 115.5 | 128 | 140.5 |
| $1/r^2$ $mm^{-2}$ ($10^{-5}$) | 12.21 | 9.43 | 7.50 | 6.10 | 5.07 |
| $e_\theta$(microstrain) | 26 | 32 | 34 | 38 | 53 |
| $e_r$(microstrain) | -8 | -11 | -17 | -25 | -37 |
| $\sigma_\theta$(N/mm$^2$) | 5.39 | 6.56 | 6.61 | 6.97 | 9.58 |
| $\sigma_r$(N/mm$^2$) | -0.046 | -0.32 | -1.55 | -3.12 | -4.82 |

Table 11: values of hoop and radial stress versus radius at penetration depth 0.73

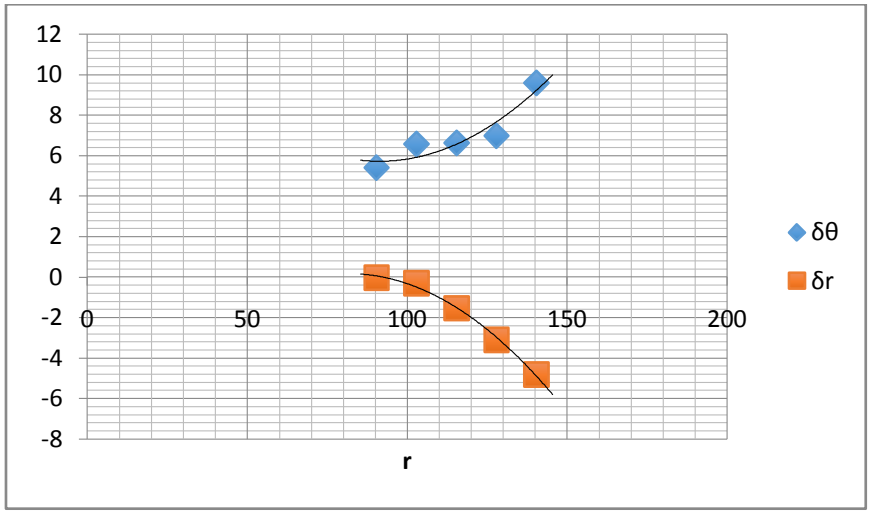


Figure 11: graph of Hoop and Radial Stress versus Radius

International Journal of Advances in Engineering and Management (IJAEM)
Volume 3, Issue 7 July 2021, pp: 1279-1289 www.ijaem.net ISSN: 2395-5252

| Depth mm | 0.7 | 1.44 | 2.19 | 2.97 | 3.91 |
|---|---|---|---|---|---|
| eθmicrostrain | 26 | 56 | 92 | 132 | 183 |
| ermicrostrain | -8 | -19 | -30 | -47 | -62 |

Table 12: Values of Hoop and Radial strain with Depth

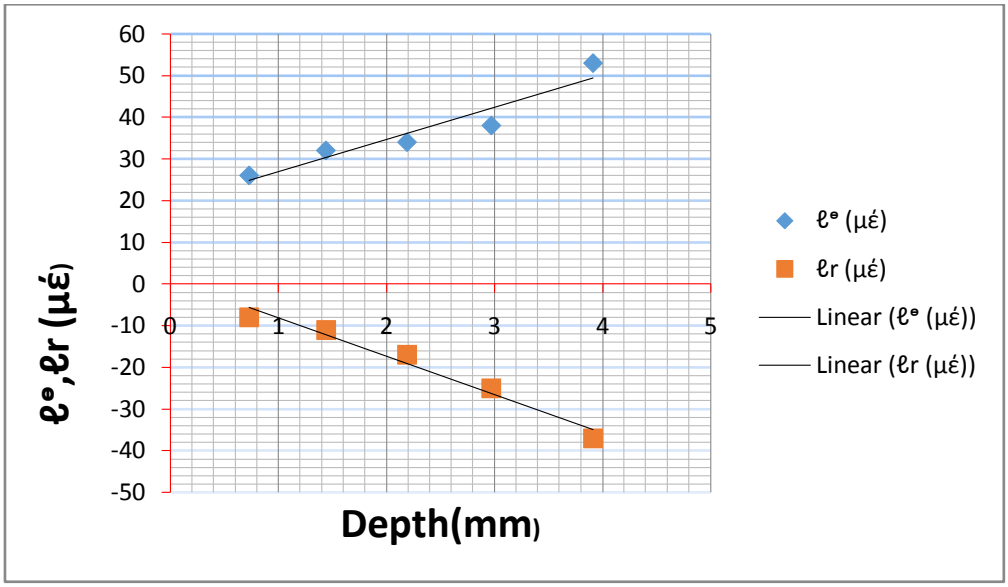


Figure 12: Graph of Hoop and Radial strain versus Depth of penetrations

## IV. DISCUSSION

The values obtained from the strain gauge readings versus plug penetration shows that the radial strain increases negatively with respect to increase in depth of penetration. The negative sign (-) in the radial readings was due to pressure acting on the surface of cylinder towards a point from opposite sides because it is compression. Whereas, the hoop or circumferential strain increases positively as the depth of penetration increases, this was as a result of tensile stress acting away from the inner towards the outer part of the cylinder. It shows that more pressure is exerted at the circumference of the cylinder, leading to the expansion of its wall, increase in volume and penetration depth.

In the graph of hoop and radial stress versus radius, at an internal pressure, the radial stress in the inner radius is equal to minus due to the pressurization of the surface cylinder and zero at the outer surface. The hoop stress which is positively pressurized is maximum at the inner surface, lower, but not zero at the unpressurised outer surface and also larger in magnitude than the radial stress. This means that both stresses occurred at the bore of the cylinder.

The values of A and B obtained from the δθ and δr against $1/r^2$ plot generally shows a progressive increase in both values from the lowest penetration depth to the highest, as showed in table 7 above. This means that as intercept A increases B also increases. In deduction, the relationship between A and B are directly proportional to the inverse of $r^2$ ($1/r^2$).

Comparing the values of A and B obtained from the graph with the calculated values of A and B using the internal pressure, p derived from the graph. At an internal pressure p, of -7.6, the values of A and B from the graph is 3.1 $N/mm^2$ and 60860N, and that of calculated values are 2.67$N/mm^2$ and 61683N, this shows a slightly different between the graph values and calculated values. The graphical and calculated values of A and B increases symmetrically with an increase of internal pressure, p. This means that it changes linearly with the applied internal pressure. So, internal pressure is directly proportional to the applied stress. It can also be said that the results obtained from the two techniques are in good agreement.

In the ideal situation both graphical and calculated values of A and B supposed to have the

same intercept and magnitude of slope, in which the only disparity would be the slope sign, but this was not the case, as there could be an experimental or calculated error arising from the experiment, such errors as:

Poor instrumental readings or error due to parallax

Improper lubrication of the plug

Apparatus not properly calibrated

However, the calculated error percentages of both A and B are within the permissible range

**5.1CONCLUSION**.

The investigation of the stress distribution in a thick-walled cylinder with internal pressure was carried out and estimated, using the numerical and analytical methods. Compressive stress was found and varies or has a maximum value of internal pressure at the inner radius and zero value at the outer radius. The tangential or hoop stress shows a maximum increase at the inner radius which leads to the expansion of the thick-walled cylinder and also increases the internal pressure with velocity of flow. However, circumferential stress is never zero at the outer radius.

The results obtained from the two techniques are in fairly good agreement. This proves that the half model used for the stress analysis is providing satisfactory results and can be used for analysis of the cylinder with internal crack. The percentage error of both A and B calculated are within the permissible range of 15%.

**5.2 RECOMMENTION:**

Haven done the above research work on the stress distribution in a thick-walled cylinder with internal pressure, I therefore, recommend that further research work be carried out to compare with already existing work done on the above subject matter, by comparing the errors encountered during the analysis.

## REFERENCE:

[1]. Annaratone, D., (2010):Pressure Vessel Design. Springer-Verlag Berlin and Heidelberg GmbH & Co. K.

[2]. Dunn, D. J. (n.d.).Complex Stress. Retrieved 10/03/ 2021, from Free Study: www.freestudy.co.uk

[3]. Hearn, E. J., (1977):Mechanics of materials 1, An introduction to the mechanics of elastic and plasticdeformation of solids and structural material. Warwick: Butterworth-Heinemann.

[4]. Jaeyoung Lee, W. R., (2012):Determining wall thickness for deepwater pipelines. Retrieved 10/ 03/ 2021, from Offshore: http://www.offshore-mag.com

[5]. Kadir, A., (n.d.). (2014):Distribution Lecture Notes (MSc in Petroleum and Gas Engineering and Management). Salford: School of Computing, Science and Technology.

[6]. Nascimento, V., (2009): Analysis of asymmetric radial deformation in pipe with local wall thinning under internal pressure using strain energy method. Brazilian Society of Mechanical Sciences and Engineering, ISBN 978-85-85769-43-7, 1.

[7]. Pressure Vessels. (n.d.). Retrieved 10/03/2021, from ETBX: www.fea-optimization.com